Physica Medica 45 (2018) 88–92

Contents lists available at ScienceDirect

Physica Medica

journal homepage: www.elsevier.com/locate/ejmp

Original paper

# Prediction of GTV median dose differences eases Monte Carlo re-prescription in lung SBRT

D. Dechambre[a,*], L.Z. Janvary[b], N. Jansen[a], P. Berkovic[c], C. Mievis[a], V. Baart[a], S. Cucchiaro[a], A.P. Coucke[a], A. Gulyban[a]

[a] Liege University Hospital, Department of Radiation Oncology, Liège, Belgium
[b] Debrecen University Hospital, Department of Radiation Oncology, Debrecen, Hungary
[c] University of Leuven, Department of Oncology, Leuven, Belgium

ARTICLE INFO

*Keywords:*
CyberKnife
Lung SBRT
Monte-Carlo re-prescription
Predictive nomogram
GTV median dose

ABSTRACT

*Background and Purpose:* The use of Monte Carlo (MC) dose calculation algorithm for lung patients treated with stereotactic body radiotherapy (SBRT) can be challenging. Prescription in low density media and time-consuming optimization conducted CyberKnife centers to propose an equivalent path length (EPL)-to-MC re-prescription method based on GTV median dose. Unknown at the time of planning, GTV D50% practical application remains difficult. The current study aims at creating a re-prescription predictive model in order to limit conflicting dose value during EPL optimization.

*Material and Methods:* 129 patients planned with EPL algorithm were recalculated with MC. Relative GTV_D50% discrepancies were assessed and influencing parameters identified using wrapper feature selection. Based on best descriptive parameters, predictive nomogram was built from multivariate linear regression. EPL-to-MC OARs near max-dose discrepancies were reported.

*Results:* The differences in GTV_D50% (median 10%, SD: 9%) between MC and EPL were significantly ($p < .001$) impacted by the lesion's surface-to-volume ratio and the average relative electronic density of the GTV and the GTV's 15 mm shell. Built upon those parameters, a nomogram ($R2 = 0.79$, SE = 4%) predicting the GTV_D50% discrepancies was created. Furthermore EPL-to-MC OAR dose tolerance limit showed a strong linear correlation with coefficient range [0.84–0.99].

*Conclusion:* Good prediction on the required re-prescription can be achieved prior planning using our nomogram. Based on strong linear correlation between EPL and MC for OARs near max-dose, further restriction on dose constraints during the EPL optimization can be warranted. This a priori knowledge eases the re-prescription process in limiting conflicting dose value.

## 1. Introduction

Robotic stereotactic radiation therapy has the potential to deliver highly conformal dose distribution with sub-millimeter accuracy. While originally designed for intra-cranial treatment, the use of the CyberKnife (CK; Accuray, Sunnyvale, CA), an image-guided frameless stereotactic radiotherapy system consisting in a lightweight 6-MV linear accelerator mounted on a robotic arm, was successfully extended to the treatment of extracranial targets [1–3]. Thanks to its tumor tracking ability compensating for lesion motion [4], early-stage non-small cell lung cancer (NSCLC) were treated by CK with favorable local control and survival rate [5]. Even though the known limitation of dose calculation in low density media [6], treatments generally prescribed 3 fractions of 20 Gy to the 80% isodose encompassing the PTV using equivalent path length algorithm (EPL) or similar solutions without lateral electron transfer calculation. With the increasing calculation capacities more advanced algorithms were available to improve accuracy with acceptable computation time. For CK in 2005, the release of voxel-based Monte Carlo dose engine (MC) with the use of variance reduction techniques [7] met the former requirements and provided superior accuracy compared to EPL especially for lung stereotactic body radiotherapy (lung SBRT) [8,9]. Nevertheless, using MC for direct prescription and optimization did not spread widely, mainly due to the difficulties to prescribe dose in a low density media and the still time-consuming optimization. Alternatively, CK centers developed various EPL-to-MC re-prescription methods. The two main propositions came from Rotterdam [10] and Lille [11] with respectively PTV_D95% and GTV_D50% re-prescription using the differences between EPL and MC.

* Corresponding author.
*E-mail address:* ddechambre@chu.ulg.ac.be (D. Dechambre).

https://doi.org/10.1016/j.ejmp.2017.12.002
Received 18 August 2017; Received in revised form 8 November 2017; Accepted 3 December 2017
Available online 19 December 2017

In both approaches, the prescription dose varied based on tumor size and location. While PTV_D95% is coping with the ICRU 50 [12] and 83 [13] norms, GTV_D50% allows for reduced variability between different cases [14]. Even though centers are adapting their prescription dose based on the average MC-recalculated GTV median dose, location and tumor size, the re-prescription amount is yet unknown at the time of optimization. This could potentially lead to problems where after re-prescription and re-calculations, tolerances to the organs-at-risk (OARs, [15]) are exceeded. In our current study, we aim to evaluate the magnitudes of EPL-to-MC discrepancies and their impact on OARs dose, followed by the creation of a predictive model to estimate EPL-to-MC differences prior to the optimization. This tool might allow to better prepare the treatment planning for lung SBRT using the CK.

## 2. Materials and methods

### 2.1. CyberKnife Monte Carlo model

Monte Carlo algorithm is represented by a single photon source located at the target location of the CyberKnife treatment head and assumed to be cylindrically symmetrical. Knowing the energy spectrum (determined from percentage depth dose), the fluence (from collimator-free profile at maximum-dose depth) and the source distribution (from in-air output factors), the beam phase space is reconstructed and used as source input for the Monte Carlo dose calculations in the patient geometry. The MC model was created according to the manufacturer specifications in an iterative process and its commissioning was the object of a previously published paper [16].

### 2.2. Management of heterogeneities within MultiPlan

In MultiPlan, the delivered dose is calculated by assuming the effective depth as determined by the density variation along the beam's path by "tracing" the beam as it travels through the tissue for EPL, while the MC associates the physical density of each voxel to a material type. This material type is used to define the photon mean free path type at a reference density as a function of photon energy. Local voxel mass density is used to scale each step of the energy deposition from each particle track. Air, soft-tissue and bone materials are represented in the system and associated to specific mass-density range.

### 2.3. Dataset and statistical analysis

One hundred and twenty-nine patients with lung lesions were included in this investigation. All treatments were performed with CyberKnife between 2010 and 2012. Lesion characteristics are listed in Table 1.

A high-resolution grid ($512^3$) was used for both EPL and MC calculations (2% uncertainty). All EPL to MC re-calculation maintained the number of beams and their monitor units. Differences in GTV_D50% between the two algorithms were assessed. For each lesion, the following variable were considered as potentially influencing those discrepancies: volume, location in the lung (both peripheral/central and island/edge), surface-to-volume ratio (SVR), average relative electronic density (RED) and the average RED of a 5 and 15 mm shells around the lesion (GTV_shell).

Best representative parameters were selected via a wrapper feature selection procedure, similar to the methodology of Nalbantov G. et al. [17], and used as inputs for the prediction model. This feature selection method was performed in WEKA (Waikato Environment for Knowledge Analysis, [18]) using a 10-fold cross validation with correlation coefficient and root mean squared error set as performance criterion. Predictive nomogram of GTV median dose differences was built upon multivariate analysis results over the selected parameters. Uni- and multivariate linear regression coefficients were reported as well as model statistical significance using an F-test at p-value $< .05$.

Differences in OAR dose tolerance values were assessed using the 3 and 5 fractions stereotactic dose constraints proposed by Timmerman RD et al. [15]. As those tolerances were defined based on simple heterogeneity correction algorithm (e.g. EPL), correlation between EPL and MC recalculated OARs dose values were evaluated following the Supplementary Material provided by the work of the Rotterdam team [10]. Coefficient of determination ($R^2$) were reported.

**Table 1**
Distribution of the lesions population characteristics by location.

| | Peripheral tumor | Central tumor | Total group |
|---|---|---|---|
| Total | 102 | 34 | 136 |
| < 5cc | 64 (47%) | 11 (8%) | 75 |
| > 5cc | 38 (28%) | 23 (11%) | 61 |
| GTV volume (cc) | 7.28[0.37–54.39] | 14.8[0.69–46.58] | 9.21[0.37–54.39] |
| SVR ($cc^{-1}$) | 7.28[2.32–54.39] | 3.77[2.16–7.18] | 4.54[2.16–8.78] |
| GTV RED | 0.85[0.3–1.05] | 1.00[0.79–1.09] | 0.89 [0.3–1.09] |
| GTV_shell (5 mm) RED | 0.41[0.15–0.85] | 0.65[0.27–1.03] | 0.47[0.15–1.03] |
| GTV_shell (15 mm) RED | 0.46[0.19–0.88] | 0.62[0.31–1.02] | 0.50[0.19–1.02] |

## 3. Results

Fig. 1 summarizes the GTV median dose discrepancies between the two algorithms. EPL and MC showed average GTV_D50% of 63.7 (standard deviation SD: 11.3) Gy and 55.2 (SD: 9.3) Gy respectively. Monte Carlo differences relative to EPL algorithm were on average of −12.5 (SD: 9.1, [1–27])%

Univariate and multivariate analysis: all parameters were found to be statistically significant factors in univariate logistic regression analysis (Table 2). The wrapper-based feature selection resulted in the following subset of variables, which were used as input in the multivariate model: Surface-to-volume ratio (SVR), average relative electronic density of GTV and of a 15 mm shell around the GTV. The three selected parameters showed highly statistically significant ($p < .001$) influence on the GTV_D50% differences.

The resulting nomogram for the multivariate model is presented in Fig. 2. Correlation coefficient (R) of 0.89 was obtained, which shows a very strong positive linear correlation ($|R| > 0.8$).

GTV median dose differences calculated for our patient cohort was on average 12.6 (SD: 8.7) vs 12.6 (SD: 7.8)% for the predictions. Their comparison is shown on Fig. 3.

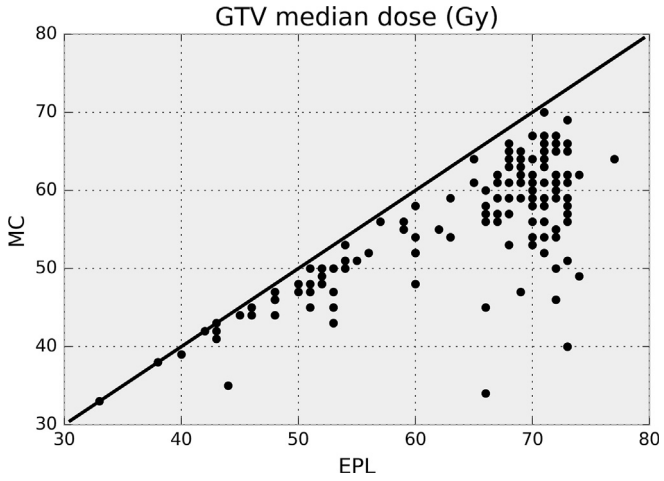


**Fig. 1.** Distribution of GTV median dose calculated using EPL and Monte Carlo dose calculation algorithms. Points on the straight line show no dose calculation algorithm differences.

**Table 2**
Results for univariate and multivariate logistic regressions for all variables and selected variables based on the wrapper approach. Dependent variables: GTV median dose differences between equivalent path length and Monte Carlo algorithms. Abbreviations: S.E. standard error, n.a not applicable, SVR surface-volume ratio, RED relative electronic density.

| Variable | Univariate | | | Multivariate: all variables | | | Multivariate: selected variables | | |
|---|---|---|---|---|---|---|---|---|---|
| | Coefficient | S.E. | p-value | Coefficient | S.E. | p-value | Coefficient | S.E. | p-value |
| Volume (cc) | −0.35 | 0.06 | <.0001 | −0.009 | 0.04 | .84 | n.a | n.a | n.a |
| SVR ($cc^{-1}$) | 3.59 | 0.40 | <.0001 | 1.41 | 0.36 | .0002 | 1.34 | 3.60 | <.0001 |
| Central/peripheral | 9.35 | 1.56 | <.0001 | −0.45 | 1.10 | .69 | n.a | n.a | n.a |
| Island/Edge | 8.82 | 1.59 | <.0001 | −0.64 | 1.26 | .61 | n.a | n.a | n.a |
| GTV_Shell (5 mm) RED | −35.53 | 2.79 | <.0001 | 1.05 | 6.67 | .87 | n.a | n.a | n.a |
| GTV_Shell (15 mm) RED | −33.77 | 3.26 | <.0001 | −18.51 | 7.10 | .01 | −19.78 | 2.32 | <.0001 |
| GTV RED | −48.14 | 3.31 | <.0001 | −28.64 | 3.85 | <.0001 | −29.15 | 3.29 | <.0001 |
| | | | | $R^2$ | S.E | p-value | $R^2$ | S.E | p-value |
| Model Performance | | | | 0.80 | 4.02 | <.0001 | 0.79 | 4.08 | <.0001 |

"Gray shade" cells indicate statistical significance at p-value < .05.

OARs dose constraint values calculated with both algorithms showed strong positive linear correlation with nearly unit determination coefficient. Differences in close-to-maximum dose tolerance values of 1% were found for the heart, great vessels and cord, of 2% for the oesophagus, 5% for the ribs and 16% for the trachea (Table 3).

Applying the Lille's re-prescription scheme to all patient plans according to lesion size and location, mean re-prescription percentage needed was 4.1 (SD: 8.2)%. Using the nomogram, the average difference between predicted and actual re-prescription amount was 0.004 (SD: 4.0)%.

## 4. Discussion

For the clinical introduction of the lung SBRT, one crucial requirement is the accurate dose calculation during treatment planning. Having MC-based calculation engine might give sufficient confidence in the simulated results. However, direct optimization in low density regions is still problematic, especially when considering the CyberKnife's narrow field overlap. As result of the rebuild-up effect, type B-optimized plans (e.g. MC) show target over-dosage when the GTV is moving inside the PTV margin. Therefore monitor units are best calculated using the type A algorithm, e.g. EPL.

In our investigation we confirm that EPL-to-MC differences in low density media might be clinically relevant (cf. Fig. 1) as EPL tends to overestimate the delivered dose by an average of 10–15% [10,19,20]. As recently shown for unresectable hepatic oligorecurrences in our department [21], such discrepancies might potentially decrease tumor control probability and are believed to be even more pronounce in the lung [22]. Thus using a re-prescription based on the MC recalculation is a viable option. This approach allows for more robust plans with less inter-plan variability (< 10%) [14], especially if the EPL-to-MC re-prescription is based on the GTV median dose. While Lacornerie T. et al. [14] offers different Monte Carlo re-prescription dose level based on location and size of the lesion, the practical application of this paper

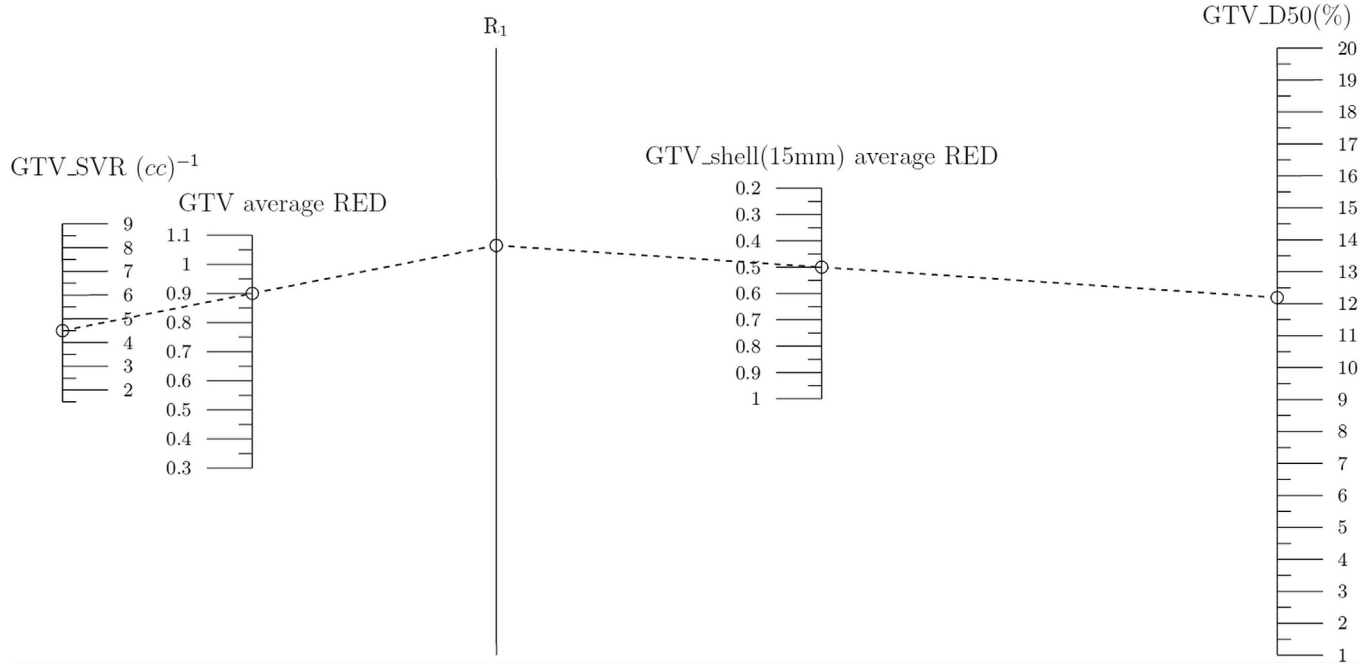


**Fig. 2.** Predictive nomogram of EPL-to-MC differences in GTV median dose using the GTV's surface-to-volume ratio, and the average relative electronic density of both GTV and GTV's 15 mm shell as input parameters. The dotted line represents a hypothetic 0.9 RED lesion presenting a GTV_SVR of 4.5$cc^{-1}$ in a GTV_shell (15 mm) of 0.5 average RED environment leading to predicted EPL-to-MC GTV_D50% differences of about 12.2%.

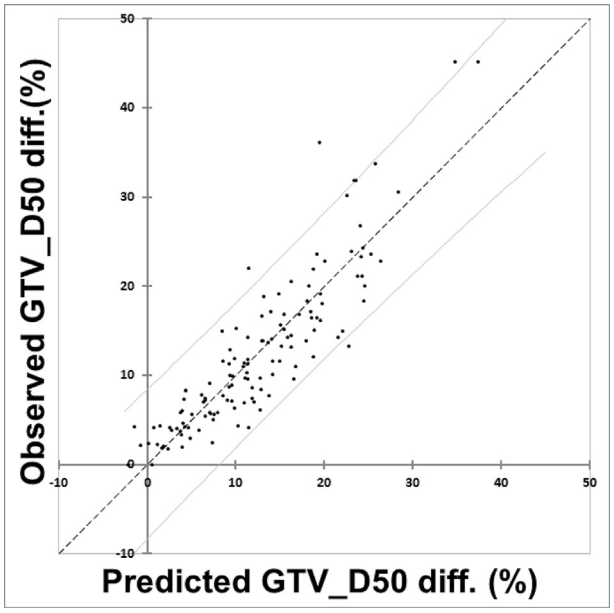


**Fig. 3.** Prediction of GTV median dose differences versus observations. Points on the dotted line shows exact predictions cases, with the two straight lines representing the 95% confidence interval.

**Table 3**
Correlation between EPL and MC recalculated OARs dose tolerance values (D10cc represent the dose received by at least 10cc of the organ). Slope factor and coefficient of determination ($R^2$) are presented for each organ.

| | Heart D10cc | Great Vessels D10cc | Cord D0.25 cc | Esophagus D5cc | Rib D5cc | Trachea D4cc |
|---|---|---|---|---|---|---|
| Slope factor | 0.99 | 0.99 | 0.99 | 0.98 | 0.95 | 0.84 |
| $R^2$ | 1 | 1 | 1 | 1 | 1 | 0.99 |

remains difficult due to OAR dose limit exceeded when re-prescribing. To anticipate the amount to re-prescribe, a predictive nomogram (cf. Fig. 2) was built using a three parameters-based linear regression.

To identify the best indicators of algorithm-induced dose differences, the impact of several variables were investigated. As bases of the Lille's dose re-prescription scheme, including parameters accounting for the GTV's location and size was mandatory.

### 4.1. Volumetric part

To express the impact of the lesion's size, GTV's volume and surface-to-volume ratio (SVR) were tested. The GTV_SVR expresses in a single value both the size and shape of the GTV. A large GTV_SVR would show the presence of tiny spikes that will considerably increase the surface while maintaining the same volume. Hence, it somehow reflects the collimator strategy involved in the planning as it will express any deviation from a spherical volume (lowest ratio). As such, it depicts the increased lack of lateral electronic equilibrium associated with the small collimator field sizes used to conformably irradiate the possible GTV's spicules.

### 4.2. Lesion location

To investigate the impact of the lesion location and by extension its direct environment, various parameters were tested such as central/peripheral and island/edge classifications [23] and the average relative electronic density of a 5 and 15 mm shell around the GTV.

On one hand, the island/edge concept extends the definition proposed by Zhuang et al. [24] where lesion is considered as an edge case if the distance between the GTV and the chest wall is inferior to 1 cm and or if the lesion if closer than 2 cm from the proximal bronchial tree (centrally located lesion definition). Otherwise, the lesion was considered as an island. This definition allowed to sort lesions by their proximity to soft-tissues as it directly influence the lack of electronic equilibrium in the air-tumor interface due to increased range of electrons in the low-density lung. On the other hand the central/peripheral classification that was historically created in function of radiotherapy-induced adverse events does not apprehend the inherent differences between calculation algorithms. While most of the peripheral lesions are also categorized as island, the edges-one close to the chest wall and high density structures such as the ribs are prone to less calculations discrepancies. In comparison, the shell density feature of 5 and 15 mm, transposed using the methodology from Zheng D et al. [25], has the advantage over the two categorizer parameters to be non-binary. Moreover it describes in a single criterion the lesion vicinity as it samples isotropically and therefore better represents the location information related to target dose calculation uncertainty.

Finally, due to the increased photon fluence created by less attenuation of the low-density tissues, the GTV average RED completes lung lesions description as the model already describes the lesion's size, shape and close environment. The resulting model involves only the most influencing parameters: GTV_SVR (R = 0.6), GTV (R = 0.81) and GTV_Shell (15 mm) average RED (R = 0.68). It shows overall good performance with a 0.78 adjusted determination coefficient and regression standard error (SE) of 4.1%. The model is believed to be GTV-delineation guidelines independent as every aspect of the tumor volume is taken into account: shape, size and density. Hence, GTV delineation inconsistencies that are likely to include more lung tissues would be taken into account.

Several studies identified parameters such as the lesion's volume and location to largely influence type A-to-type B (e.g. EPL-to-MC) algorithm differences but few actually tried to model them. Zheng D. et al. [25] identified the PTV volume and the density of a 2 mm thick PTV shell as most predictive factors of type A-to-type B PTV D95% deficiency. They found no model improvement when adding other variables like PTV, GTV, and lung mean density or PTV margin. While reporting significance factor, no model determination coefficient was available to evaluate the proportion of observation it explained. To compare the performance of the models, the average normalized root mean square of errors (RMSE) between data and predictions was calculated. We report a RMSE score of 0.089 versus their calculated 0.091 for their multiple linear regression model. Meaning that our prediction are slightly closer to the observed values. While they observed high correlation between PTV D95 and GTV D95, their work was built upon an internal target volume (ITV) concept. It implies that more low-density lung tissue would be present into the PTV volume leading to higher type A-to-type B discrepancies. Furthermore, the larger collimator size used to irradiate the PTV will decrease the effect of electronic disequilibrium. Hence causing less dose discrepancies inside the GTV.

While highly impacting the target dose, effects on organ-at-risk were evaluated as well. As presented in Table 3, all the dose constraints calculated with EPL and MC algorithm showed a nearly perfect linear correlation with < 2% dose discrepancies on most OAR except for the rib and the trachea that presents 5 and 16% respectively. For the purpose of comparison, mean dose difference to OAR were calculated and found similar to the near-max dose reported. While not often used due to highly localized treatment, mean homo-lateral lung (including the PTV) dose (MLD) linear coefficient of 0.87 ($R^2$ = 0.96) was obtained using a similar methodology as before. Zheng et al. [25] (dynamic conformal arc) and Liu H. et al. [26] (IMRT) confirmed our finding stating that the dose differences for the OARs and normal tissues were relatively small (within 3%) and negligible. While our results agree within 3% for the lung, rib and trachea, all other mean organ dose calculated by Van der Voort van Zyp et al. [10] (Supplementary Data)

shows EPL-to-MC differences of 11%. Additional scarce data were gathered for the MLD with type A-to-type B linear coefficient of 0.99 (3D-CRT), 0.95 (dynamic conformal arc) and 0.93 (3D-CRT) reported by respectively Schushell et al. [19], Zhuang et al. [23] and Altunbas C. et al. [27]. While the previously cited study used different treatment delivery technique, no correlation could be established with type A-to-type B OARs dose discrepancies.

Nevertheless, all studies showed a linear relationship between the two classes of dose calculations for OARs. Based on this conditions, the nomogram for re-prescription becomes a valuable tool. Following the proposition of the Lille CK group, knowledge of the EPL-to-MC differences that are likely to be observed allows to adapt the planning beforehand by lowering OARs dose tolerances prior to the EPL-based treatment planning optimization. It eases the re-prescription process and limits the likelihood of conflicting dose values between the target and the surrounding organs for CyberKnife lung SBRT.

The strengths of the our nomogram are the availability of its planning strategy-independent parameters and its intrinsic simplicity to use which makes it suitable for the clinical routine. As consequence, performances of the model are directly impacted. In an attempt to improve the model, one should consider post-treatment planning parameter such as beams configuration. Those consisting mostly of anterior beam are likely to increase the magnitude of dose discrepancies in the posterior part of the target due to the CyberKnife inability to treat from the rear.

Finally, the results might be influenced by parameters specific to our plans. As CyberKnife only treats with 6 MV flattening filter free (FFF) beams, using higher energy would results in larger target dose differences where the opposite effect would occur when using flattened fields. While the quantitative model from our study may not directly apply to clinical cases with the above-mentioned delivery specificity, our proposed methodology is easily transferable and applicable to other data sets involving any type A-to-type B dose calculation algorithm differences. However, the multivariate coefficient obtained on Table 2 are dependent on the user settings such as the treatment platform, the treatment planning system (TPS), the dose calculation algorithms and even further on the machine and MLC modelling in the TPS.

## 5. Conclusion

The differences in GTV median dose between MC and EPL is significantly impacted by the lesion's surface-to-volume ratio and average relative electronic density of both GTV and GTV's 15 mm shell. Build upon those three parameter, our nomogram is able to predict the GTV_D50% discrepancies. As EPL-to-MC OAR dose tolerance limit proved to have a strong linear correlation (conversion factors range [0.84–0.99]), the a priori knowledge of the re-prescription amount might be used during the EPL optimization, easing the re-prescription process in limiting conflicting dose value.

## References


[1] Chang JY, Senan S, Paul MA, Mehran RJ, Louie AV, Groen HJM, et al. Stereotactic ablative radiotherapy versus lobectomy for operable stage I non-small-cell lung cancer: a pooled analysis of two randomised trials. Lancet Oncol 2016;16:630–7. http://dx.doi.org/10.1016/S1470-2045(15)70168-3.Stereotactic.

[2] Bezjak A. RTOG 0813: Seamless Phase I/Ii Study of Stereotactic Lung Radiotherapy (SBRT) for Early Stage, Centrally Located, Non-Small Cell Lung Cancer (NSCLC) in Medically Inoperable Patients. 2011.

[3] Timmerman RD, Michalski J, Fowler J, Choy H, Johnstone D, Galvin JM, et al. Radiation therapy oncology group RTOG 0236 A Phase II Trial of Stereotactic Body Radiation Therapy (SBRT) in the Treatment of Patients with Medically Inoperable Stage I / II Non-Small Cell Lung Cancer. 2004;6.

[4] Harada K, Katoh N, Suzuki R, Ito YM, Shimizu S, Onimaru R, et al. Evaluation of the motion of lung tumors during stereotactic body radiation therapy (SBRT) with four-dimensional computed tomography (4DCT) using real-time tumor-tracking radiotherapy system (RTRT). Phys Medica 2016;32:305–11. http://dx.doi.org/10.1016/j.ejmp.2015.10.093.

[5] Janvary ZL, Jansen N, Baart V, Devillers M, Dechambre D, Lenaerts E, et al. Clinical outcomes of 130 patients with primary and secondary lung tumors treated with Cyberknife robotic stereotactic body radiotherapy. Radiol Oncol 2017;51:178–86. http://dx.doi.org/10.1515/raon-2017-0015.

[6] Search H, Journals C, Contact A, Iopscience M. Address IP. Collapsed cone and analytical anisotropic algorithm dose calculations compared to VMC + + Monte Carlo simulations in clinical cases. J Phys Conf Ser 2007;21007. http://dx.doi.org/10.1088/1742-6596/74/1/012007.

[7] Kawrakow I, Fippel M. Investigation of variance reduction techniques for Monte Carlo photon dose calculation using XVMC. Phys Med Biol 2000;45:2163–83. http://dx.doi.org/10.1088/0031-9155/45/8/308.

[8] Toutaoui A, Ait chikh S, Khelassi-Toutaoui N, Hattali B. Monte carlo photon beam modeling and commissioning for radiotherapy dose calculation algorithm. Phys Medica 2014;30:833–7. http://dx.doi.org/10.1016/j.ejmp.2014.05.007.

[9] Ma C-M, Mok E, Kapur A, Pawlicki T, Findley D, Brain S, et al. Clinical implementation of a Monte Carlo treatment planning system. Med Phys 1999;26:2133–43. http://dx.doi.org/10.1118/1.598729.

[10] van der Voort van Zyp NC, Hoogeman MS, van de Water S, Levendag PC, van der Holt B, Heijmen BJ, et al. Clinical introduction of Monte Carlo treatment planning: a different prescription dose for non-small cell lung cancer according to tumor location and size. Radiother Oncol 2010;96:55–60. http://dx.doi.org/10.1016/j.radonc.2010.04.009.

[11] Bibault JE, Mirabel X, Lacornerie T, Tresch E, Reynaert N, Lartigau E. Adapted prescription dose for monte carlo algorithm in lung SBRT: clinical outcome on 205 patients. PLoS One 2015;10. http://dx.doi.org/10.1371/journal.pone.0133617.

[12] Prescribing, Recording, and Reporting Photon-Beam Intensity-Modulated Radiation Therapy (IMRT): J ICRU 2010;10:NP.3-NP. doi: http://dx.doi.org/10.1093/jicru/ndq002.

[13] Program C, Quantities F, Quality I, Ion-beam R. The International commission on radiation units and measurements. J ICRU 2010;10:NP.2-NP. doi: http://dx.doi.org/10.1093/jicru/ndq001.

[14] Lacornerie T, Lisbona A, Mirabel X, Lartigau E, Reynaert N. GTV-based prescription in SBRT for lung lesions using advanced dose calculation algorithms. Radiat Oncol 2014;9:223. http://dx.doi.org/10.1186/s13014-014-0223-5.

[15] Timmerman RD. An overview of hypofractionation and introduction to this issue of seminars in radiation oncology. Semin Radiat Oncol 2008;18:215–22. http://dx.doi.org/10.1016/j.semradonc.2008.04.001.

[16] Dechambre D, Baart V, Cucchiaro S, Ernst C, Jansen N, Berkovic P, et al. Commissioning Monte Carlo algorithm for robotic radiosurgery using cylindrical 3D-array with variable density inserts. Phys Med 2017;33:152–8. http://dx.doi.org/10.1016/j.ejmp.2017.01.005.

[17] Nalbantov G, Kietselaer B, Vandecasteele K, Oberije C, Berbee M, Troost E, et al. Cardiac comorbidity is an independent risk factor for radiation-induced lung toxicity in lung cancer patients. Radiother Oncol 2013;109:100–6. http://dx.doi.org/10.1016/j.radonc.2013.08.035.

[18] Kohavi R, John GH. Wrappers for feature subset selection. Artif Intell 1997;97:273–324. http://dx.doi.org/10.1016/S0004-3702(97)00043-X.

[19] Schuring D, Hurkmans CW. Developing and evaluating stereotactic lung RT trials: what we should know about the influence of inhomogeneity corrections on dose. Radiat Oncol 2008;3:21. http://dx.doi.org/10.1186/1748-717X-3-21.

[20] Rassiah-Szegedi P, Salter BJ, Fuller CD, Blough M, Papanikolaou N, Fuss M. Monte Carlo characterization of target doses in stereotactic body radiation therapy (SBRT). Acta Oncol 2006;45:989–94. http://dx.doi.org/10.1080/02841860600919225.

[21] Berkovic P, Gulyban A, Nguyen PV, Dechambre D, Martinive P, Jansen N, et al. Stereotactic robotic body radiotherapy for patients with unresectable hepatic oligorecurrence. Clin Colorectal Cancer 2016. http://dx.doi.org/10.1016/j.clcc.2017.03.006.

[22] Berkovic P, Gulyban A, Swenen L, Dechambre D, Viet Nguyen P, Jansen N, et al. EP-1226: Stereotactic robotic body radiotherapy for patients with pulmonary oligometastases. Radiother Oncol 2017;123:S661–2. http://dx.doi.org/10.1016/S0167-8140(17)31661-4.

[23] Zhuang T, Djemil T, Qi P, Magnelli A, Stephans K, Videtic G, et al. Dose calculation differences between Monte Carlo and pencil beam depend on the tumor locations and volumes for lung stereotactic body radiation therapy. J Appl Clin Med Phys 2013;14:4011. http://dx.doi.org/10.1120/jacmp.v14i2.4011.

[24] Zhuang T, Djemil T, Qi P, Magnelli A, Stephans K, Videtic G, et al. Dose calculation differences between Monte Carlo and pencil beam depend on the tumor locations and volumes for lung stereotactic body radiation therapy. J Appl Clin Med Phys 2013;14:38–51. http://dx.doi.org/10.1120/jacmp.v14i2.4011.

[25] Zheng D, Zhu X, Zhang Q, Liang X, Zhen W, Lin C, et al. Target dose conversion modeling from pencil beam (PB) to Monte Carlo (MC) for lung SBRT. Radiat Oncol 2016;11:83. http://dx.doi.org/10.1186/s13014-016-0661-3.

[26] Liu H, Zhuang T, Stephans K, Videtic G, Raithel S, Djemil T, et al. Dose differences in intensity-modulated radiotherapy plans calculated with pencil beam and Monte Carlo for lung SBRT. J Appl Clin Med Phys 2015;16:5514. http://dx.doi.org/10.1120/JACMP.V16I6.5514.

[27] Altunbas C, Kavanagh B, Dzingle W, Stuhr K, Gaspar L, Miften M. Dosimetric errors during treatment of centrally located lung tumors with stereotactic body radiation therapy: Monte Carlo evaluation of tissue inhomogeneity corrections. Med Dosim 2013;38:436–41. http://dx.doi.org/10.1016/j.meddos.2013.06.002.